Nov 5th, 12:00 AM - 12:00 AM

Finite Element Analysis of Cold-Formed Dimpled Steel Columns

V. B. Nguyen

M. A. English

M. A. Castellucci

Twenty-Second International Specialty Conference on Cold-Formed Steel Structures
St. Louis, Missouri, USA, November 5 & 6, 2014

Finite Element analysis of cold-formed dimpled steel columns

V.B. Nguyen[1], M.A. English[2] and M.A. Castellucci[3]

Abstract

Dimpled steel products are produced from the combination of an innovative dimpling process and a traditional forming process such as cold-roll forming or press-braking. The wider use of cold-formed dimpled steel members has promoted considerable interest in the local instability and strength of these members. Of particular interest is their buckling behaviour and ultimate strength capacity. However, the dimpling process produces cold-formed sections with a complex 'dimpled' surface topography and the 'dimpled' material is non-uniformly work hardened through the entire thickness. Owing to these complex issues, there are no existing methods to calculate the buckling strength of the dimpled products and validate against physical measurements. This paper presents a Finite Element analysis of the compressive behaviour of cold-formed dimpled steel columns. True stress-strain data obtained from physical tests were incorporated into nonlinear simulations of dimpled steel columns. The simulation results were compared with compression test results on dimpled channel and lipped channel columns and good agreements in both buckling and ultimate strength were obtained. It is demonstrated that the Finite Element analysis can therefore be used to analyse and design cold-formed dimpled steel columns.

[1]Research Engineer, Hadley Industries plc, Smethwick, West Midlands, UK and University of Wolverhampton, Wolverhampton, West Midlands, UK.
[2]Design and Development Manager, Hadley Industries plc, Smethwick, West Midlands, UK.
[3]Technical Director, Hadley Industries plc, Smethwick, West Midlands, UK.

Introduction

Dimpled steel strips are cold-roll formed from plain steel strips by the UltraSTEEL® process developed by Hadley Industries plc. The process uses a pair of rolls with rows of specially shaped teeth that form the dimple shapes from both sides of the plain sheet (Nguyen et al. 2012a). The dimpled strip is then progressively formed into a desired shape by passing through a series of cold-rolled forming rolls, arranged in tandem, or by press braking. It has been proven through physical tests and numerical simulations that the strength of dimpled specimens was significantly greater than plain specimens originating from the same coil material, and this enhancement is a result of the cold work applied to the material during the dimpling process (Collins et al. 2004, Nguyen et al. 2011, 2012a, 2013 and 2014).

Dimpled steel products are increasingly used in a wide range of light building construction. They include wall studs, framing and roofing members, corrugated panels, vineyard posts, windows and door reinforcement and many other products. Amongst them, channel shaped products are the most common and widely used as compression and bracing members in such applications. The wider use of cold-formed dimpled steel members has promoted considerable interest in the local instability and strength of these members. Of particular interest is their buckling behaviour and ultimate strength capacity. However, design criteria for compressive strength of such cold-formed dimpled steel members have not been available. In a recent study (Nguyen et al. 2012b), semi-empirical expressions for determining buckling and ultimate strengths of component plate elements of plain and dimpled channel columns were formulated based on experimental data. Owing to the complex surface topography and the material which is highly nonlinear through the entire thickness, analytical methods are incapable of solving the post-buckling of dimpled steel members. Numerical methods such as Finite Element (FE) analysis, however, have been shown to be suitable for solving the complex and interrelated nonlinear changes in contact, geometry and material properties that occur in the process and section forming of dimpled steel products (Nguyen et al. 2013, 2014). This enables the development of an efficient FE model to represent buckling and post-buckling of dimpled steel products.

In this paper, FE simulations of the compressive behaviour of cold-formed dimpled steel channel and lipped channel columns were presented. This includes a summary of the simplified approach to practically represent the dimpling process and resultant dimpled section which was earlier proposed by Nguyen et al. (2013). Simulations of plain steel columns having the same nominal dimensions and original material properties with dimpled columns were also carried out in order to further evaluate the simulation results and effects of the dimpling process on structural properties of dimpled columns. The test programme reported previously (Nguyen et al. 2012a, 2012b) were summarised and results were used to verify the performance of the FE simulations.

Finite Element analysis

Finite Element simulations were conducted using Marc (MSC Software, version 2012) to simulate the UltraSTEEL® dimpling process and compression tests of dimpled channel and lipped channel columns. The simplified approach in Nguyen et al. (2013) was used to practically represent dimpled columns. This approach can be summarised as following steps: (i) simulating a simplified dimpling process that deform a flat steel plate into a dimple, (ii) use this generic dimple geometry to generate dimpled strip- in this study, a dimpled column is a very large FE model so shell element approach instead of 3-D element approach is applied. It should be noted that only the geometry of the dimple is transferred from the dimpling process in step (i), material properties of the dimple is given from a separate tensile test on a dimpled steel sample, (iii) simulating the cold forming process that develop the dimpled strip into a desired dimpled column (iv) simulating the dimpled column subject to compression test. The simulations of plain steel products were carried out in parallel with dimpled steel products in order to further evaluate the FE results and effects of the dimpling process. In these simulations, the material properties of the sheet steel were obtained from physical tensile tests. A parametric study was carried out to investigate the effects of several parameters to the reliability of the FE model and results. Based on this investigation, a set of appropriate parameters were selected as presented in Nguyen (2012c).

Geometric and material nonlinearity that occurred within the model were taken into account, thereby effectively modelling large strains and rotations. An elastic-plastic material model was used for the sheet steel. The material has a Young's modulus E of 205 GPa and a Poisson's ratio of 0.3. Marc requires the input of the material stress-strain data in the form of true stress (σ_{true}) versus true plastic strain (ε^p_{true}). The true stress and true plastic strain were converted from the engineering stress (σ_{nom}) and engineering strain (ε_{nom}) as follows:

$$\sigma_{true} = \sigma_{nom}(1 + \varepsilon_{nom}) \qquad (1)$$

$$\varepsilon^p_{true} = \ln(1 + \varepsilon_{nom}) - \sigma_{nom}/E \qquad (2)$$

The engineering stress and strain data of the plain and dimpled steel was obtained from the tensile tests, and shown in Figure 1.

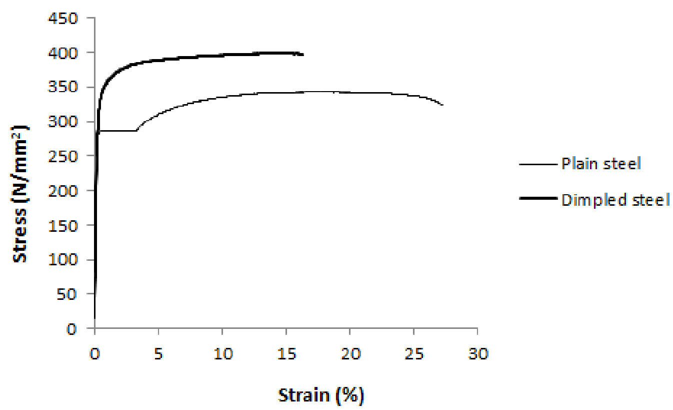

Figure 1 Engineering stress-strain curves of the plain and dimpled sheet steels

The plain sheet was deformed into the dimple. The dimple geometry was then used as a 3-D generic part to generate dimpled sheets or sections. As a section contains corners, other simulations were carried out to deform the dimple to generate corner elements, i.e. of 90^0 bend angle as illustrated in Nguyen et al. (2013). Using a 3-D solid element approach, the model contained more than ten million elements which would be impractical to process. To simplify the modelling procedure, shell elements were used instead of 3-D solid elements. In the column test simulations, all stresses and strains were set to zero at the beginning of the analysis.

In this example, the channel column specimens had a length of 500 mm, thickness of 0.90 mm, flange width of 50.80 mm, web width of 101.06 mm and corner radius of 1.30 mm. The lipped channel column specimens had a length of 500 mm, thickness of 1.95 mm, lip width of 13.50 mm, flange width of 50.60 mm, web width of 100.60 mm and corner radius of 4.00 mm. Other column specimens had dimensions and material properties as presented in Nguyen et al. (2012a, 2012b). Therefore, the dimple had to be presented by shell elements on its central plane. Figure 2 illustrates the column specimens generated from the generic dimpled elements and the model setup including boundary conditions at the column ends.

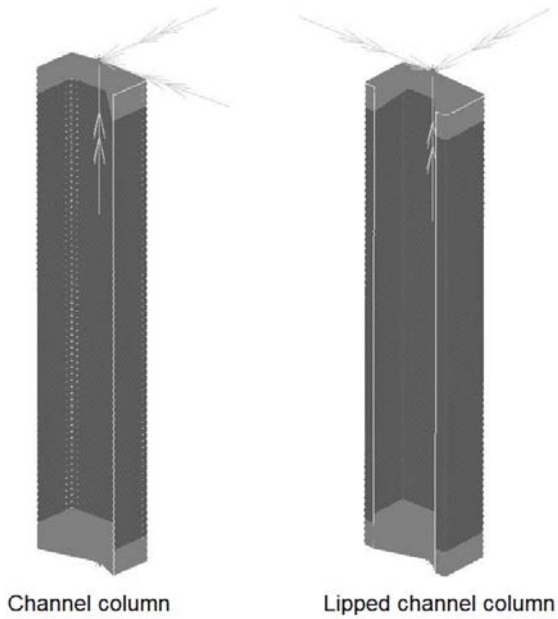

Figure 2 FE models of the dimpled column specimens using shell elements and its boundary conditions to model the column ends

The simulations were carried out on channel and lipped channel column specimens, fixed at both ends. The dimpled channel column was modelled using 472,500 elements while the dimpled lipped channel column was modelled using 578,250 elements; they are four-node, thin-shell elements with global displacements and rotations as degrees of freedom (element type 139). Load was applied on the top end of the column using the displacement-controlled method. The loading point was at a reference node that connects to a set of tied nodes at the end of the column, as shown in Figure 2. The link between the reference node and the tied nodes was based on a rigid link connection, only unrestrained in loading direction. The displacement was increased in successive increments until the column failed. A full Newton-Raphson method was used for the iterative procedure and an implicit, static analysis was employed.

Simulations of the column compression test undertaken in two steps. In the first step, a linear elastic buckling analysis was performed on the perfect column to obtain its buckling mode shapes (eigenvalues). In the second step, a nonlinear post-buckling analysis was carried out to predict the column behaviour and ultimate load capacity. The buckling shapes derived in the first step were used as initial geometric imperfections of the column specimen. In these simulations, the lowest buckling modes were used to generate the imperfections because they are usually the critical buckling modes (Moreyra and Peko 1994).

The mode and degree of initial imperfections were selected as suggested in Nguyen et al. (2013). The degree of initial imperfection was specified as the maximum amplitude of the buckling mode shape and there were several ways to determine it. According to EN 1993-1-5: 2006, Annex C, Section C.5 (British Standard 2006), the geometric imperfection values applied to finite element models have to be a/200 (a is the web width) for local buckling. Schafer and Pekoz (1998) suggested for type 1 local imperfection: $d1 \approx 0.006w$, and for type 2 local imperfection: $d2 \approx t$; where type 1 is the maximum local imperfection in a stiffened element ($w/t < 200$, $t < 3$ mm); type 2 is the maximum local imperfection in an unstiffened element ($w/t < 100$, $t < 3$ mm); w is the width and t is the thickness. The imperfection values were also defined in terms of thickness, such that Yap and Hancock (2006) used the imperfection values 0.15t and 0.64t and Chou et al. (2000) tested 0.10t, 0.50t and 1.00t. These values were used in FE modelling and the results were compared with the test results. It was found that 0.10t imperfection value produced the best agreement with the test result in terms of buckling and ultimate loads; therefore, the imperfection value of 0.10t was adopted in this study.

FE results and experimental validation

A calibrated 200-kN capacity test rig was used for the column compression tests. Figures 5 and 6 illustrate the experimental setup for testing of a dimpled column specimen. The column specimen was placed in the test rig and was loaded at a constant rate of 0.11 mm/min.

A detailed test programme that related to the arrangement of strain gauges and displacement transducers (LVDTs), specimen calibration, measurements, test setup, support end conditions, alignment procedure, instrumentation for determining buckling load and test procedure was described in Nguyen et al. (2012a, 2012b). The data of plain and dimpled column specimens was used in FE simulation and the results were summarised.

FE results and experimental validation

Figure 3 shows the comparison between the experimental and FE load-axial displacement curves for plain and dimpled channel columns. The comparison between the experimental and FE load-axial displacement curves for plain and dimpled lipped channel columns are illustrated in Figure 4. The experimental curves were also plotted for comparison.

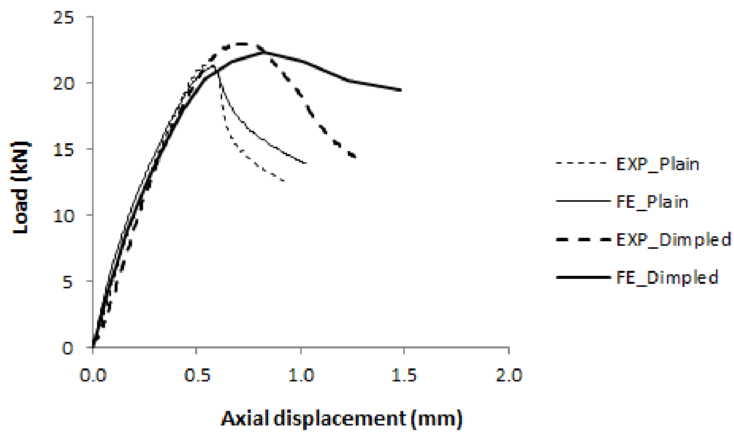

Figure 3 Load-axial displacement curves of plain and dimpled channel columns

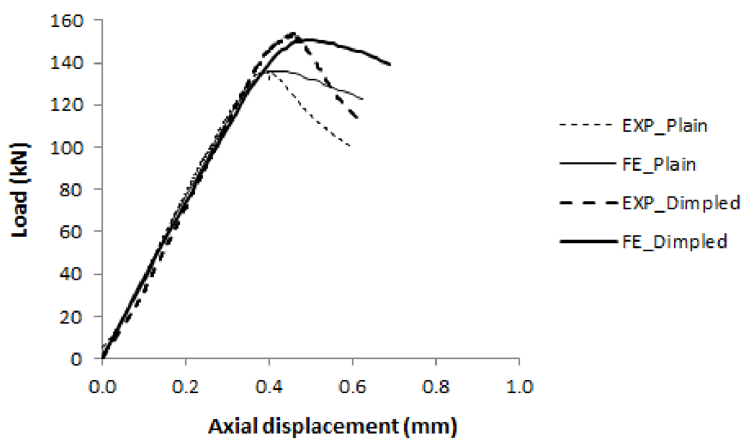

Figure 4 Load-axial displacement curves of plain and dimpled lipped channel columns

The FE predicted values for both channel and lipped channel columns were in good agreement with the experimental values, with a maximum difference of 10%. In addition, the initial stiffness and behaviour predicted by the simulation are in very good agreement with the experimental results for both plain and dimpled specimens. It can be seen that the experimental curves are associated with less loads in post-peak behaviour. Lesser load could be due to some degree of imperfection occurred during failure, which is difficult to measure and apply in FE modelling.

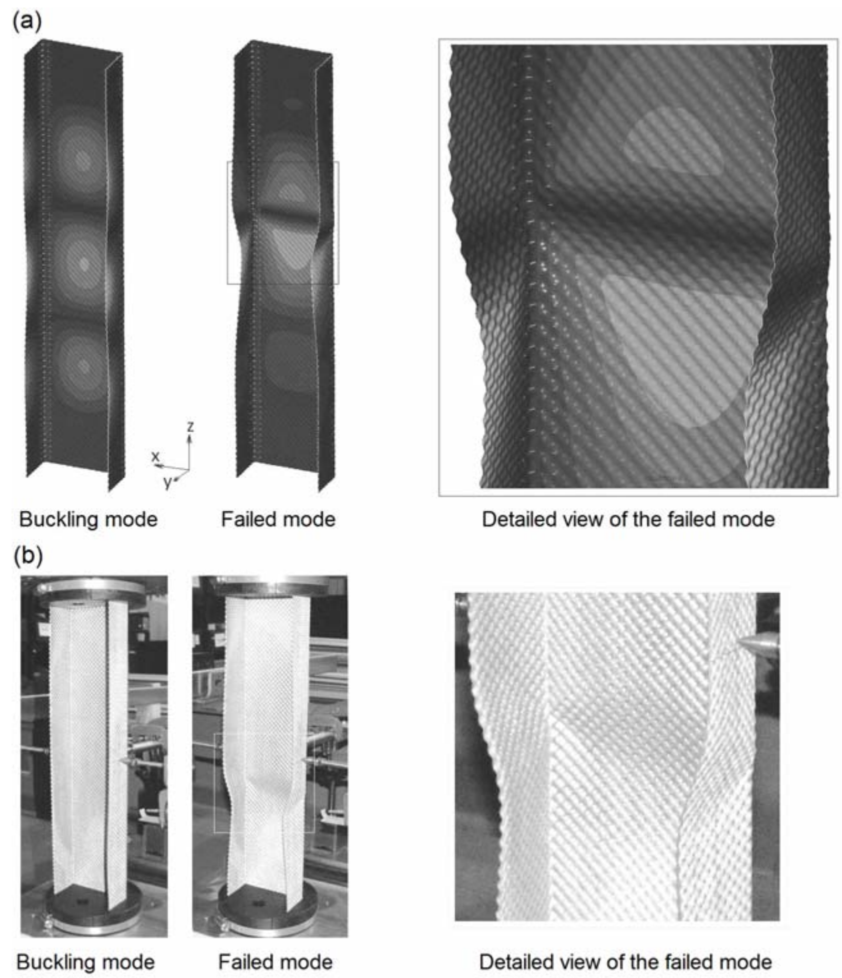

Figure 5 Buckling and failed mode shapes of the dimpled channel column (a) FE results, and (b) experimental results. Displacement contour is presented in FE results in which lighter colours indicate greater displacement magnitudes.

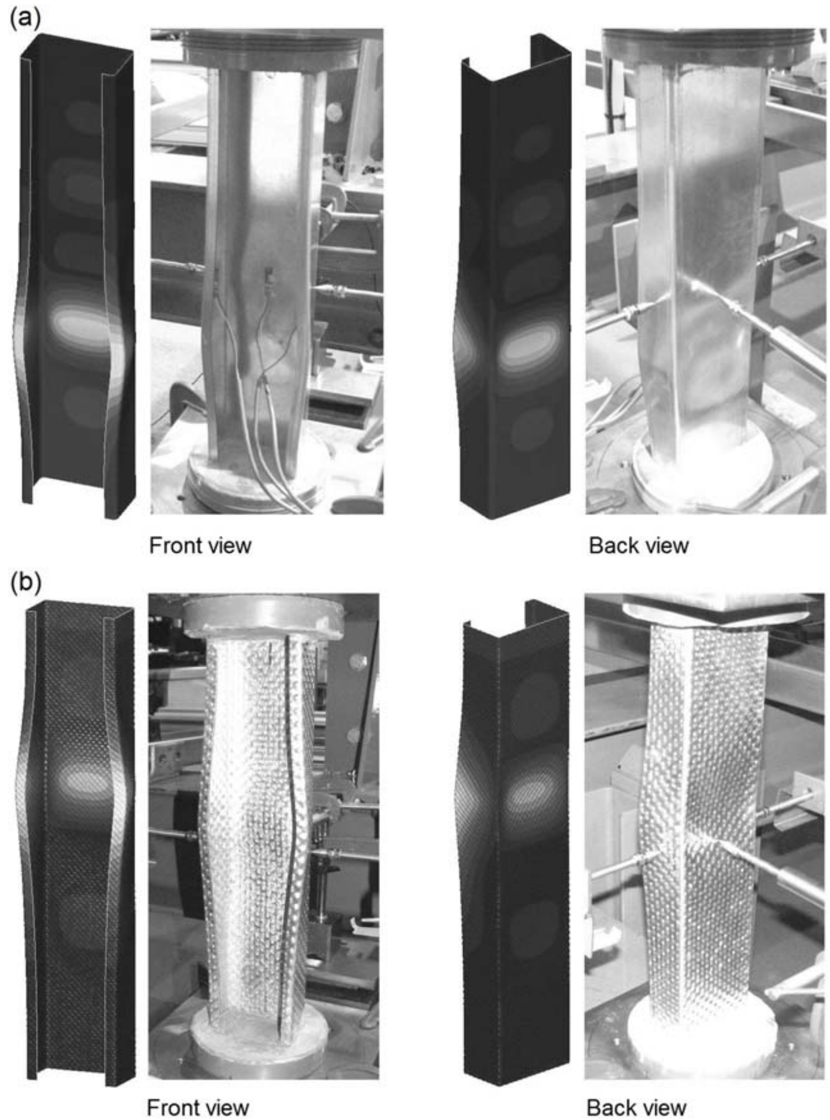

Figure 6 FE and experimental results of failed mode shapes (a) plain lipped channel column, and (b) dimpled lipped channel column. Both front view and back view are displayed. Displacement contour is presented in FE results in which lighter colours indicate greater displacement magnitudes.

Figure 5 shows the buckling and failed mode shapes of the dimpled channel column in comparison with the experimental shapes. Figure 6 shows the failed mode shapes of the plain and dimpled lipped channel columns, in which the experimental shapes were also illustrated. It can be seen that the buckling and failed modes predicted by FE models are very similar to the experimental modes for both plain and dimpled column specimens. This further confirms the validation of the FE simulations.

It was observed from the FE simulations that the columns remained elastic at the initial loading level. At local buckling, the axial stiffness reduced with the following stiffness getting smaller until the ultimate load was reached. After that point, the load decreased but the column specimens still exhibit substantial load bearing capacity. As the load increases it was observed that wavelike deflections appeared along the length of the flanges and webs of the column specimens, as shown in Figures 5 and 6. These column specimens clearly exhibited 'local buckling' and due to this local collapse, they failed at maximum loads which had lower magnitudes than yield loads. It can be seen from Figures 5 and 6 that the plain and dimpled column specimens had similar failure modes; they developed the same plastic mechanism in failure, in the form of lip-disc mechanisms (Dubina and Ungureanu 2000).

For a broader validation, results of FE buckling load P_{cr_FE} and ultimate load P_{mL_FE} of channel column specimens which were tested previously (as presented in Nguyen et al. 2012a, 2012b) and comparison with experimental results are presented in Table 1. Test groups 1 and 5-8 contain only plain specimens. The column specimens were labelled, a plain specimen label starts with the letter 'P' whilst a dimpled specimen starts with the letter 'U'. The material properties were determined from tensile tests of plain and dimpled specimens. Compared to the plain column specimens from the same groups, the buckling and ultimate loads were increased by 9-33% and 8-26% in the dimpled column specimens, respectively. The significant increase in the strengths of dimpled columns is a result of the cold work applied to the material during the dimpling process.

The elastic buckling loads predicted by the FE simulation were compared with the test results (the mean values are presented) as shown in column (7) of Table 1. The FE and experimental values were similar, with a maximum difference of 16% and 19% for test groups 4-8 and 10-14, respectively; however, the FE values were significantly greater than the experimental ones and the difference was great as 34% and 37% for test groups 1-3 and 9, respectively. The FE ultimate loads were compared with the experimental ultimate loads, as shown in column (8) of Table 1. The FE simulations provided conservative predictions of the experimental results, with a maximum difference of 5% for test groups 4-8 and 11% for test groups 10-14; however, the FE ultimate values were underestimated the experimental values and the difference was great as 51% and 21% for test groups 1-3 and 9, respectively. It was noted that for the specimens in test groups 1-3 and 9, the theoretical local buckling loads were even greater than the full section yield loads. The main reason for this could be the fact that these columns buckled in inelastic region while the FE local buckling loads were evaluated by means of elastic analysis.

Conclusion

The FE analysis of cold-formed dimpled steel channel and lipped channel columns subject to compression tests were conducted to investigate their compressive strengths. FE modelling details that related to the model setup, material properties and selecting initial imperfection values were described. The FE results were verified against a series of column compression tests available from the authors' previous studies. FE models for cold-formed plain steel columns which originated from the same coil material with dimpled columns were also carried out to further evaluate the performance of the FE simulations.

The FE results of compression tests of plain and dimpled columns were in good agreement with the experimental results, further indicating that the dimpling process and products was accurately represented by the FE model. For dimpled columns, the increase in the strength was observed in FE simulations and was satisfactorily validated by experimental tests. The increase in strength of the dimpled specimens is a result of the plastic deformation developed throughout the thickness of the dimpled sheet, during the dimpling process.

The validation of FE models presented in this paper indicates that they can be used as an alternative and complementary method to predict the buckling and ultimate strength of dimpled steel columns with high accuracy. On-going work includes using the FE approach present here to analyse more dimpled steel columns of different geometries, and to formulate design expressions to predict the strength of dimpled steel columns under compression.

Table 1 FE results and comparison with experimental values. * Data given in Nguyen et al. (2012a); ** Data given in Nguyen et al. (2012b); [a] Comparison is presented as column ()/column (). For example, the comparison in column (7) is presented as (3)/(5) which compares the experimental buckling load in column (3) against the FE buckling load in column (5)

Test group	Specimen	Experiment		FE simulation		Comparison	
		P_{cr} (kN)	P_{mL} (kN)	$P_{cr\ FEA}$ (kN)	$P_{mL\ FEA}$ (kN)	(3)/(5)	(4)/(6)
(1)	(2)	(3)	(4)	(5)	(6)	(7)	(8)
1*	P-T1.5F29.6W101.6L500	34.89	43.07	43.90	41.08	0.79	1.05
2*	P-T0.9F15.0W44.7L200	14.69	14.69	21.85	9.76	0.67	1.51
	U-T0.9F15.0W44.7L200	17.34	17.34	26.08	12.19	0.66	1.42
3*	P-T1.5F30.4W70.0L500	44.29	46.00	54.34	34.27	0.82	1.34
	U-T1.5F30.4W70.0L500	48.25	50.34	57.12	47.02	0.84	1.07
4*	P-T1.0F50.8W101.6L500	7.14	21.14	7.94	21.17	0.90	1.00
	U-T1.0F50.8W101.6L500	8.80	22.90	9.54	22.33	0.92	1.03
5**	P-T1.5F50.8W101.6L500	30.96	47.73	36.06	50.50	0.86	0.95
6**	P-T1.5F38.1W76.2L500	36.92	44.49	40.91	44.90	0.90	0.99
7*	P-T0.8F31.0W51.7L200	7.36	14.05	8.76	13.77	0.84	1.02
8*	P-T0.8F38.0W51.7L200	6.65	14.84	7.96	14.35	0.84	1.03
9*	P-T1.2F24.5W32.0L200	22.44	22.83	35.73	20.82	0.63	1.10
	U-T1.2F24.5W32.0L200	25.81	26.04	26.94	21.60	0.96	1.21
10*	P-T1.2F32.5W32.0L400	19.48	20.42	23.38	22.55	0.83	0.91
	U-T1.2F32.5W32.0L400	25.81	25.81	30.80	23.50	0.84	1.10
11*	P-T1.2F38.0W32.0L400	16.01	22.04	19.69	24.55	0.81	0.90
	U-T1.2F38.0W32.0L400	19.80	26.95	24.30	24.94	0.81	1.08
12*	P-T1.2F46.0W32.0L400	14.53	23.98	16.29	26.25	0.89	0.91
	U-T1.2F46.0W32.0L400	16.84	27.88	18.70	26.54	0.90	1.05
14*	P-T1.2F55.0W32.0L500	11.99	24.09	13.18	27.22	0.91	0.89
	U-T1.2F55.0W32.0L500	14.54	26.92	13.98	27.76	1.04	0.97

References

Chou SM, Chai GB, Ling L. Finite element technique for design of stub columns. Thin-Walled Structures 2000;37:97-112.

Collins J, Castellucci MA, Pillinger I, Hartley P. The influence of tool design on the development of localised regions of plastic deformation in sheet metal formed products to improve structural performance. In: Proc. 10th International Conference on Metal Forming; 2004. Paper no. 68.

Dubina D, Ungureanu V. Elastic-plastic interactive buckling of thin-walled steel compression members. In: Proceedings of the 15th International Specialty Conference on Cold-Formed Steel Structures. 2000. p.223-237.

European Standard EN 1993-1-5: 2006/AC: 2009. Europe Code 3 - Design of steel structures - Part 1-5: Plate structural elements. Brussels: European Committee for Standardization; 2009.

Hadley Industries plc, PO Box 92, Downing Street, Smethwick, West Midlands, B66 2PA, UK.

Moreyra ME, Peko T. Finite element studies on lipped channel flexural members. In: Proceedings of the 12th International Specialty Conference on Cold-Formed Steel Structures. 1994. p.57-74.

Nguyen VB, Wang CJ, Mynors DJ, Castellucci MA, English MA. Finite Element simulation on mechanical and structural properties of cold-formed dimpled steel. Thin-Walled Structures 2013; 64:13-22.

Nguyen VB, Wang CJ, Mynors DJ, English MA, Castellucci MA. Compression tests of cold-formed plain and dimpled steel columns. Journal of Constructional Steel Research 2012a;69:20-29.

Nguyen VB, Wang CJ, Mynors DJ, English MA, Castellucci MA. Compressive strength tests and design of cold-formed plain and dimpled steel columns. In: Proceedings of the 21st International Specialty Conference on Cold-Formed Steel Structures. 2012b. p.127-142.

Nguyen VB, Wang CJ, Mynors DJ, English MA, Castellucci MA. Dimpling process in cold roll metal forming by finite element modelling and experimental validation. Journal of Manufacturing Processes 2014; In Press.

Nguyen VB, Wang CJ, Mynors DJ, English MA, Castellucci MA. Mechanical properties and structural behaviour of cold-rolled formed dimpled steel. Steel Research International 2011; Special Issue:1072-1077.

Nguyen VB. The UltraSTEEL® dimpling process, tension, bending and compression of dimpled steel products: FE simulation and experimental validation. Report No. KTP.O19a.12. Hadley Industries plc, Downing Street, Smethwick, West Midlands, B66 2PA, UK; 2012c.

Schafer BW, Pekoz T. Computational modelling cold-formed steel: characterizing geometric imperfections and residual stresses. Journal of Constructional Steel Research 1998;47:193-210.

Yap DCY, Hancock GJ. Interaction buckling and postbuckling in the distortional mode of thin-walled sections. Research Report no. R870, University of Sydney; 2006.